Biochemistry and Biophysics Reports 34 (2023) 101483

Contents lists available at ScienceDirect

Biochemistry and Biophysics Reports

journal homepage: www.elsevier.com/locate/bbrep

Development of the observation of membrane fusion with label-free liposomes by calcium imaging

Morihiro Hotta [a], Kengo Hayase [a], Aya Kitanaka [a], Tianshu Li [b], Shinji Takeoka [a,b,*]

[a] Department of Life Science and Medical Bioscience, Graduate School of Advanced Science and Engineering, Waseda University (TWIns), 2-2 Wakamatsu-cho, Shinjuku-ku, Tokyo, 162-8480, Japan
[b] Institute for Advanced Research of Biosystem Dynamics, Research Institute for Science and Engineering, Waseda University, 3-4-1 Okubo, Shinjuku-ku, Tokyo, 169-8555, Japan

ARTICLE INFO

Keywords:
Liposome
Cationic liposome
Membrane fusion
Calcium imaging
Peak detection

ABSTRACT

Liposomes are artificial vesicles composed of lipid bilayers that have enabled drugs to be encapsulated and delivered to tumor tissue. Membrane-fusogenic liposomes fuse with the plasma membranes of cells to deliver encapsulated drugs directly to the cytosol, which makes it a promising method for rapid and highly efficient drug delivery. In a previous study, liposomal lipid bilayers were labeled with fluorescent probes, and colocalization of labeled lipids with plasma membrane was observed under a microscope. However, there was concern that fluorescent labeling would affect lipid dynamics and cause liposomes to acquire membrane fusogenic ability. In addition, encapsulation of hydrophilic fluorescent substances in the inner aqueous phase sometimes requires an additional step of removing unencapsulated substances after preparation, and there is a risk of leakage. Herein, we propose a new method to observe cell interaction with liposomes without labeling. Our laboratory has developed two types of liposomes with different cellular internalization pathways, i.e., endocytosis and membrane fusion. We found that cytosolic calcium influx would be triggered following the internalization of cationic liposomes, and different cell entry routes led to different calcium responses. Thus, the correlation between cell entry routes and calcium responses could be utilized to study liposome-cell interactions without fluorescent labeling lipids. Briefly, liposomes were added to phorbol 12-myristate 13-acetate (PMA)-primed THP-1 cells, and calcium influx was measured by time-lapse imaging using a fluorescent indicator (Fura 2-AM). Liposomes with high membrane fusogenic ability elicited a strong transient calcium response immediately after adding liposomes, whereas those taken up mainly by endocytosis elicited multiple weak calcium responses. In order to verify the cell entry routes, we also tracked the intracellular distribution of fluorescent-labeled liposomes in PMA-primed THP-1 cells using a confocal laser scanning microscope. It was shown that for fusogenic liposomes, colocalization with plasma membrane occurred at the same time as calcium elevation, whereas for liposomes with a high endocytosis potential, fluorescent dots were observed in the cytoplasm, suggesting the cell internalization by endocytosis. These results suggested that the calcium response patterns correspond to cell entry routes, and membrane fusion can be observed by calcium imaging.

1. Introduction

Liposomes are particles composed of a lipid membrane, with diameters ranging from tens of nm to several μm. Liposomes less than 200 nm in diameter can accumulate at the tumor site due to the EPR effect [23]. Immunoliposomes can deliver inclusions to targeted tissues [22]. Therefore, immunoliposomes are useful carriers that deliver drugs to tumors, and treatment with immunoliposomes was conducted [1]. Also, liposomes are one of the representative carriers in drug delivery systems that enable intracellular delivery of bioactive substances. Liposomes are usually taken up by cells via endocytosis, which requires the substances encapsulated in the liposome to be released from endosomes to the cytosol by destabilizing the endosomal membrane. In contrast, membrane fusion of liposomal bilayer with plasma membrane allows liposome-encapsulated substances to be delivered directly to the cytosol. Therefore, intracellular delivery is thought to be more rapid and

* Corresponding author. Department of Life Science and Medical Bioscience, Graduate School of Advanced Science and Engineering, Waseda University (TWIns), 2-2 Wakamatsu-cho, Shinjuku-ku, Tokyo, 162-8480, Japan.
E-mail address: takeoka@waseda.jp (S. Takeoka).

https://doi.org/10.1016/j.bbrep.2023.101483
Received 2 December 2022; Received in revised form 31 March 2023; Accepted 2 May 2023

efficient than the endocytic pathway [2]. In previous studies, fluorescent labeling of liposomes has been used to detect membrane fusion with the plasma membrane. However, encapsulation of hydrophilic fluorescent substances in the inner aqueous phase of liposomes requires an additional step of removing unencapsulated substances when liposomes are prepared with hydration method. There is also a risk of leakage of the encapsulated substances at around 37 °C if cholesterol is not used. Using fluorescent-labeled lipids, either by conjugating a fluorescent probe to the original lipids or inserting additional fluorescent lipids into the bilayer, would change the lipid composition and affect the molecular assembling states, potentially reducing the accuracy of the measurement. Additionally, some amphiphilic fluorophores were reported to contribute to liposomes acquiring a membrane-fusogenic ability [3]. Therefore, a new method without lipid modification is highly desired, which can also help achieve high-throughput screening purposes by minimizing preparation procedures [3].

A series of cationic lipids have been developed in our laboratory. In particular, amino acid-type lipids with different hydrophobic chains were reported to have various potentials to trigger immune responses, such as the NLRP3 inflammasome activation in macrophages [4]. Cationic aminolipid is composed of a lysine (K) head group, hydrocarbon spacer, and hydrophobic fatty acids (Fig. 1). 1,5-ditetradecyl-*N*-lysyl-*N*-trityl-L-glutamate (K3C14) and 1,5-dihexadecyl-*N*-lysyl-*N*-trityl-L-glutamate (K3C16) are two carbon different in the hydrophobic chains, but they showed different cell entry routes in the form of liposomes. K3C14 liposomes are preferably introduced via endocytosis, whereas K3C16 liposomes are preferably incorporated into the cell by membrane fusion [5]. These phenomena were observed by fluorescent labeling of a small portion of lipids and revealed that K3C16 liposomes were more rapidly introduced into the cytosol compared to K3C14 liposomes [6]. K3C16 liposomes encapsulating FITC-dextran were added to HeLa cells, and FITC-dextran was observed to be transported into the cells 10 min after addition [6]. Since the two lipids have a similar structure but different cellular internalization pathways, a comparison of the two lipids is expected to provide insight into the effect of lipid structure on the cell-liposome interaction.

Calcium is an essential intracellular second messenger. In macrophages, calcium signaling involves many cellular events, such as phagocytosis, immune responses, and pseudopodia elongation [7]. In quiescent cells, cytosolic calcium levels keep low compared to that of extracellular and endoplasmic reticulum (ER) [8]. In activated cells, however, calcium influx occurs with different magnitude, responsiveness, and frequency depending on the upstream signal and activates different downstream effectors. Therefore, calcium changes over time are crucial in regulating and orchestrating different cellular events. It can be monitored using a fluorescent indicator such as Fura 2-AM, a ratio metric fluorescent dye sensing cytosolic free calcium after intracellular hydrolysis. In our previous study, we found that some cationic liposomes can promote the NLRP3 inflammasome activation in human macrophages [5] and have the potential to induce calcium influx [9]. Therefore, we are interested in further understanding how cationic liposomes affect intracellular calcium mobilization.

In this study, we hypothesize that the calcium response patterns relate to the cell entry route of liposomes, in the particular fusion of the plasma membrane with liposomes. We stimulated PMA-primed THP-1 cells with two kinds of cationic liposomes K3C14 and K3C16, and measured the intracellular calcium response to the liposomes by time-lapse fluorescence microscopy. This study aims to develop a method for screening and detecting liposomes that can fuse with plasma membranes without fluorescent modification. Therefore, it could allow us to study the mechanism of membrane fusion by changing the size and composition of fusogenic liposomes, the concentration of liposomes, the

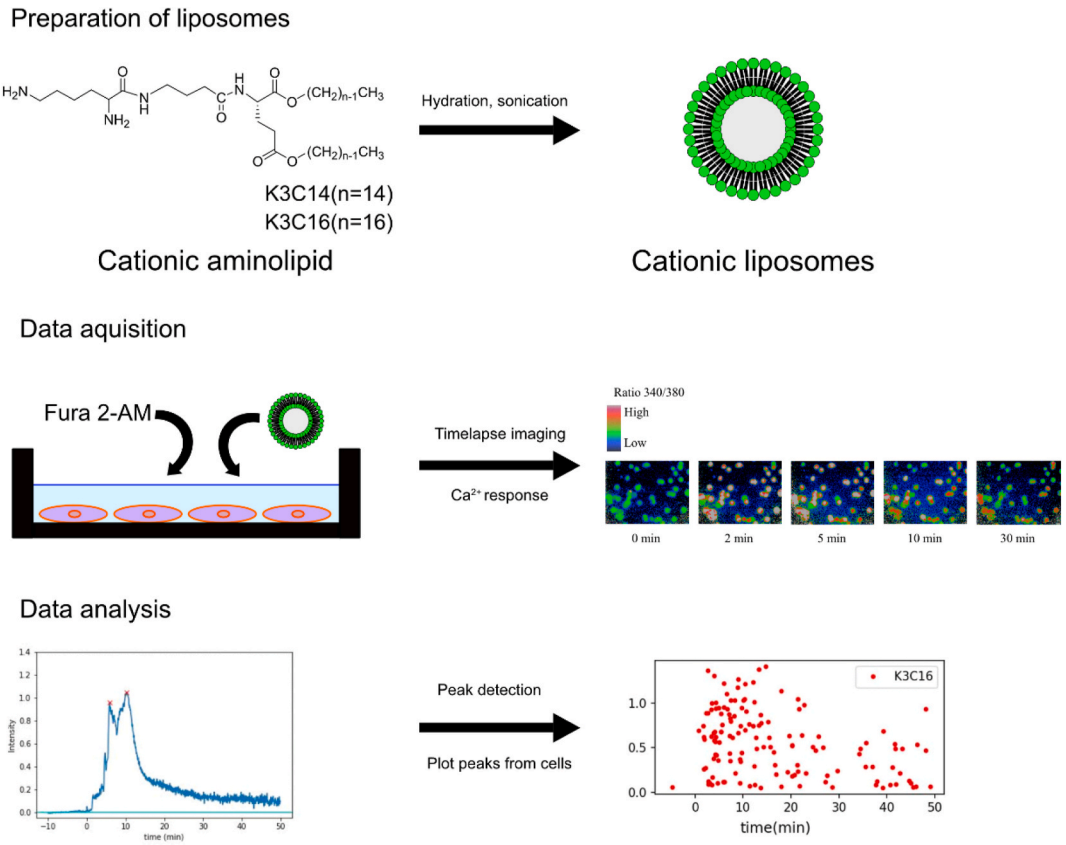

Fig. 1. Schematic illustration of this study.
Two cationic aminolipids, K3C14 and K3C16, were used to prepare cationic liposomes. Fura 2-AM was loaded to PMA-primed THP-1 cells, and cationic liposomes were applied during the time-lapse imaging. From the calcium response of the individual cells, peaks of the response were collected.

stage of the cell cycle, and the kinds of cells, and by adding various inhibitors.

2. Materials and methods

2.1. Materials

Cationic aminolipids K3C14 and K3C16 were synthesized in our laboratory [10]. Fura 2-AM was purchased from Dojindo (Kumamoto, Japan). Sonicator (US-1) was purchased from As One (Osaka, Japan). Alexa fluor 488™ NHS ester was purchased from Thermo Fisher Scientific (Massachusetts, USA). THP-1 cells were purchased from Cell Bank (Osaka, Japan). RPMI medium and PMA were purchased from Fujifilm Wako Chemicals (Osaka, Japan). DAPI was purchased from Merck KGaA (Darmstadt, Germany).

2.2. Preparation of cationic liposomes

K3C14 and K3C16 were hydrated (5 mM, 1200 rpm) at room temperature (r.t.) overnight in HEPES buffer (2 mL, 20 mM, pH 7.4). After hydration, particle size was controlled by sonication (oscillation frequency: 38 kHz, r.t., 1 h).

Particle size and zeta potential were measured using a Malvern Zetasizer ZS90. 10 μL of the sample was diluted in 990 μL of 20 mM HEPES buffer. Particle size measurement was performed by using a plastic cuvette at 25 °C with 11 runs and 3 measurements. Zeta potential measurement was done by using a capillary cell with a voltage of 20 V, 20 runs, 3 measurements at 25 °C.

2.3. Calcium response of cells stimulated by label-free cationic liposomes

THP-1 cells were cultured in RPMI medium (10% fetal bovine serum, 1% penicillin-streptomycin) in an incubator (37 °C, 5% CO_2). THP-1 cells (2.0×10^5 cells/mL, 1 mL) mixed with PMA (final concentration 100 nM) were seeded in 35 mm glass base dishes and stimulated for 18 h. After stimulation, cells were washed three times with DPBS and incubated in RPMI medium for 1 day. After washing three times with DPBS, Fura 2-AM diluted in HBS (115 mM NaCl, 5.4 mM KCl, 20 mM HEPES, 1 mM $MgCl_2$, 10 mM glucose, 2 mM $CaCl_2$) was added (37 °C, 2.5 μM, 1 mL, 10 min). After washing three times with DPBS, HBS was added at r.t. (10 min) to remove unreacted Fura 2-AM. HBS was removed, and 1 mL of fresh HBS was added. The dish was placed on an inverted fluorescence microscope (IX71, Olympus, Tokyo, Japan) with a 20x objective lens (UApo/340, 0.75, Olympus) and a CCD camera (ORCA-ER, Hamamatsu Photonics, Hamamatsu, Japan) [11]. Fura 2-AM was excited alternately every 3 s using two wavelengths (340 nm and 380 nm) of excitation light from a xenon lamp that passed through an excitation filter (FF01-340/26-25 (OPTO-LINE, Saitama, Japan) for 340 nm and MBP380 (Olympus) for 380 nm) [11–13]. The light transmitted through a beam splitter (400 nm, DM400 (Olympus)) and an emission filter (420 nm, BA420 (Olympus)) was captured by a cooled CCD camera. After 10 min of imaging, 250 μL of 500 μM liposome dispersion diluted in HBS was added to the medium (final concentration: 100 μM), and images were taken for 50 min after addition. HBS solution was used as a negative control. TI Workbench was used for image acquisition and background subtraction [13]. The area without cells was set as background and subtracted for each wavelength. ROI was set up to surround the cell, the fluorescence intensity was acquired at each excitation wavelength, and the ratio of the two fluorescence images F340/F380 was calculated. This was done for all cells in the field of view at each time point (42.0 ± 4.6 cells per field of view).

The individual calcium response was then output using python 3.9. The average ratio before the addition of liposome dispersion (from 30 s to 9 min after the start of imaging) was set to 0 and subtracted from the fluorescent intensity. The x-axis was set to time, the y-axis was set to fluorescence intensity ratio, and the upper and lower limits of the y-axis were specified as 0.6 and −0.1, respectively. The fluorescence intensity peak was then detected using SciPy (detection: height = 0.05, distance = 10, width = 10, prominence= (0.02, None)). Calcium responses were plotted as blue lines and detected peaks as red crosses. Peaks were detected in all cells under the same conditions, and the time and intensity of the peak detected in one experiment are plotted on the x and y axes, respectively. The average time and intensity of the calcium response peaks obtained from the cells in one fluorescence microscopy experiment was calculated for 3 experiments.

2.4. Fluorescence image of cells after the addition of the fluorescent-labeled liposomes

5 μL of 10 mM Alexa fluor 488™ NHS ester in DMSO was added to K3C14 and K3C16 liposomes (5 mM, 200 μL in 20 mM HEPES buffer) stirred at r.t. for 2 h to react with primary amines in lipids. After the reaction, particle size was controlled by sonication (15 min, r.t.) to obtain fluorescent-labeled cationic liposomes.

THP-1 cells (2.0×10^5 cells/mL, 1 mL) mixed with PMA (final concentration 100 nM) were seeded in 35 mm glass base dishes and stimulated for 18 h. After stimulation, cells were washed 3 times with DPBS and incubated with RPMI medium for 1 day. After washing 3 times with DPBS, fluorescent-labeled liposome dispersion diluted with HBS was added (final concentration 100 μM, 1 mL) and stimulated for 5, 10, and 30 min. The cells were then washed three times with heparin sodium dissolved in DPBS (20 U/mL) [14–16] and fixed with 4% paraformaldehyde (37 °C, 15 min), washed twice with DPBS, and stained with DAPI (300 nM, 8 min, r.t.). After washing twice with DPBS, images were acquired with a confocal microscope FV1000 (Olympus, Tokyo, Japan) (objective lens: × 40). Images were acquired with Alexa fluor 488™ and DAPI filter. Images were acquired in three different fields of view under one condition. Images were acquired with z-stack.

The intracellular dynamics of Alexa fluor 488™ were classified on the acquired cell images [6]. Each field of view contained 27.8 ± 4.9 cells. All cells in the 3 images were divided into 4 categories, and the percentages were calculated: cells with fluorescent lipids in the plasma membrane were classified as M, cells with stained cytoplasm as C, cells with both stained plasma membrane and cytoplasm as M/C, and cells with neither stained as N. This was done for each liposome and time of addition to follow the intracellular dynamics of the fluorescent lipids.

3. Results

3.1. Preparation of cationic liposomes

The particle size and zeta potential of K3C14 and K3C16 liposomes were 196 ± 3 nm, and 45 ± 1.02 mV, 204 ± 10 nm and 47.0 ± 0.06 mV, respectively (Table 1). The polydispersity index (PDI) was around 0.2, suggesting the monodispersity and little aggregation of cationic liposomes prepared by sonication. The zeta potential was above 40 mV, indicating that the liposomes were strongly positively charged [5,6]. There is no significant difference in size and zeta potential though the polydispersity is high for K3C14. PDI of liposomes increased after labeling, indicating that labeling caused some aggregation.

Table 1
Liposomes for experiment.

Lipid	Particle size (nm)	PDI (a.u.)	Zeta potential (mV)
K3C14	196 ± 3	0.219 ± 0.006	45.0 ± 1.02
K3C16	204 ± 10	0.158 ± 0.012	47.0 ± 0.06
K3C14 after labeling	249 ± 5	0.320 ± 0.001	51.5 ± 1.88
K3C16 after labeling	151 ± 1.5	0.179 ± 0.032	37.5 ± 1.19

3.2. Calcium response of cells stimulated by label-free cationic liposomes

Using Fura 2-AM as a calcium indicator, the calcium response of cells stimulated by liposomes without fluorescence labeling was observed over time under inverted fluorescence microscope (Fig. 2). The color gradient indicates the calcium concentration level; it changes from blue to red as calcium concentration increases. Usually, the color of all cells was stained blue, indicating that the intracellular calcium level was low. In cells with HBS solution, the color changed slightly before and after the solution was added. After adding the K3C14 liposome dispersion, there were few color changes, which means the intracellular calcium level did not change significantly. After a while, some cells showed small color changes, which showed the elevation of calcium level. Some others showed multiple color changes, suggesting fluctuation in calcium level (Fig. 2, white arrows). On the other hand, when K3C16 liposome dispersion was added to the cells, many cells responded to red after 2 min, indicating a strong elevation in intracellular calcium concentration (Fig. 2, yellow arrows). At 5 or 10 min after addition, the color of the cells changed back to blue, indicating that the calcium elevation is transient. It is suggested that K3C14 liposomes caused sporadic small-scale calcium oscillation, while the addition of K3C16 liposomes caused a large peak in calcium level immediately after the addition.

Although the overall trend was roughly understood, it is difficult to analyze in detail the differences in the intensity of calcium response and the response time from the images of fluorescence intensity ratio alone. We needed to analyze the changes in intracellular calcium concentration for all cells individually. The change in calcium response of a single cell was output as time on the x-axis and fluorescence intensity ratio on the y-axis (Fig. 3). Five cells of each group are shown as representative; the calcium responses of all cells in each of the three experiments with the two types of liposomes (K3C14: 114 cells, K3C16: 138 cells, negative control: 118 cells) are shown in Supplementary (Fig. S1). The red arrow indicates the time of addition of liposomes; in some cells to which K3C14 liposome dispersions were added, the small-scale elevation of the fluorescent intensity ratio frequently occurred a while after addition. On the other hand, in cells to which K3C16 liposome dispersion was added, a large peak was found immediately after addition in many cells. In some cells, the fluctuation of the ratio was additionally observed a while after addition, similar to K3C14.

We focused on the peak intensities and peak times to further analyze the calcium response. Parameters were set to detect peaks in the fluorescent ratio of individual cells, and the detected peaks are marked with a red X, as shown in Fig. S2. In this study, we spotlighted large peaks to catch the overall trend and set the conditions such that large peaks were detected. In subsequent peak detections, the conditions for peak detection were uniformly applied to all cells in one field of view of the fluorescence microscope (K3C14: 39 cells, K3C16: 47 cells, negative control: 31 cells). The detected peaks were plotted with time on the x-axis and peak intensity on the y-axis (Fig. 4). Small peaks were observed in the calcium response of cells stimulated with K3C14 liposome after 30 min. On the other hand, large peaks were observed immediately after the addition of K3C16 liposomes.

The average time and peak intensity were calculated for one experiment (Fig. S3). In addition, the average of the three experiments was obtained (Fig. 5). The K3C14 liposomes showed peaks with low intensities around 30 min after addition. On the other hand, the K3C16 liposomes showed large peaks around 15 min after addition. This indicates that the calcium response of the cells differs depending on the type of cationic aminolipid of liposomes. In addition, the small deviation of K3C16 experiments suggested a highly reproducible trend.

3.3. Fluorescence image of cells after the addition of the fluorescent-labeled liposomes

Fluorescent-labeled liposomes were added to PMA-primed THP-1 cells, fixed, DAPI-stained, and observed under confocal microscopy to clarify the distribution of liposomes when the calcium response occurred (Fig. 6). The intensity of intracellular fluorescence increased with increasing stimulation time with K3C14 liposomes. Furthermore, the fluorescence was found to exist as bright spots in the cell. On the other hand, the plasma membrane was stained in a linear pattern with strong bright spots at 5 min stimulation with K3C16 liposomes. Then, as stimulation time progressed, more cells with stained cytoplasm were observed. In cells with stained plasma membranes, cytoplasmic fluorescence was low after 5 min of stimulation. After 30 min of stimulation, a strong distribution of bright spots was observed in the cytoplasm, similar to that of K3C14.

For each stimulation time, cells were classified based on whether the fluorescent lipid was present in the cytoplasm or the plasma membrane, and the percentage of cells was calculated (Fig. 7). 5 min of stimulation with K3C14 liposomes did not introduce fluorescent-labeled lipids in more than half of the cells. As the stimulation time prolonged, the percentage of cells without fluorescence decreased, and the percentage of cells with fluorescence in the cytoplasm and plasma membrane increased. In contrast, K3C16 liposomes showed fluorescence in 80% of cells at the plasma membrane already after 5 min of stimulation. As the stimulation time increased, the percentage of cells with both cytoplasm and plasma membrane stained increased.

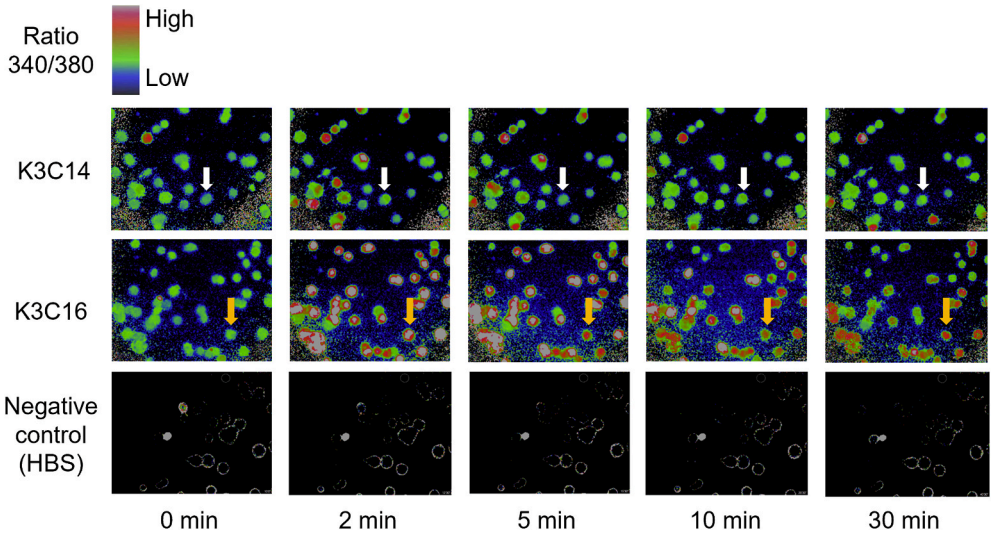

Fig. 2. Time-lapse calcium imaging of PMA-primed THP-1 cells stimulated by K3C14 or K3C16 liposomes.
The ratio of the two fluorescent images was taken, with blue to red indicating higher calcium concentrations. Fura 2-AM was introduced (2.5 μM, 10 min) into THP-1 cells primed with PMA (18 h, 100 nM). Liposomes were added (final concentration 100 μM) under fluorescence microscopy. The time in figure shows the time elapsed after the addition of liposomes. (For interpretation of the references to color in this figure legend, the reader is referred to the Web version of this article.)

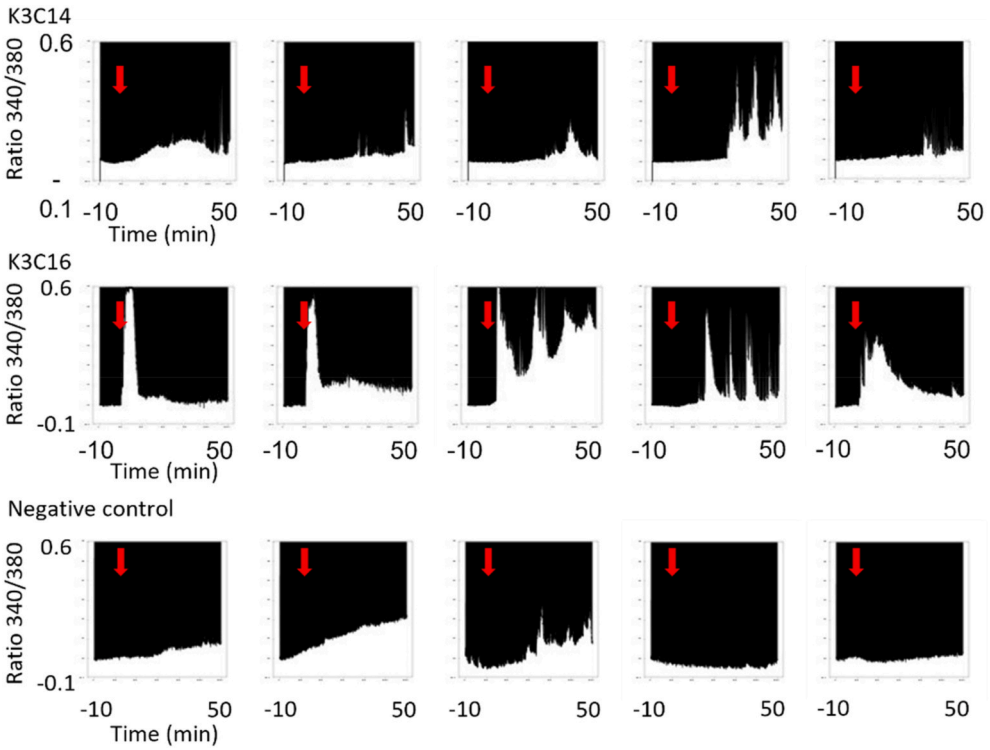

Fig. 3. Time-lapse calcium response of individual THP-1 cells.
The fluorescent intensity ratios of individual cells were measured, and five representative cells out of all cells in three experiments (K3C14: 114 cells, K3C16: 138 cells, negative control: 118 cells) are showed here. The dispersion of liposomes was added at the time indicated by the red arrow (0 min), and the ratio was monitored for 50 min after addition (final concentration 100 μM). (For interpretation of the references to color in this figure legend, the reader is referred to the Web version of this article.)

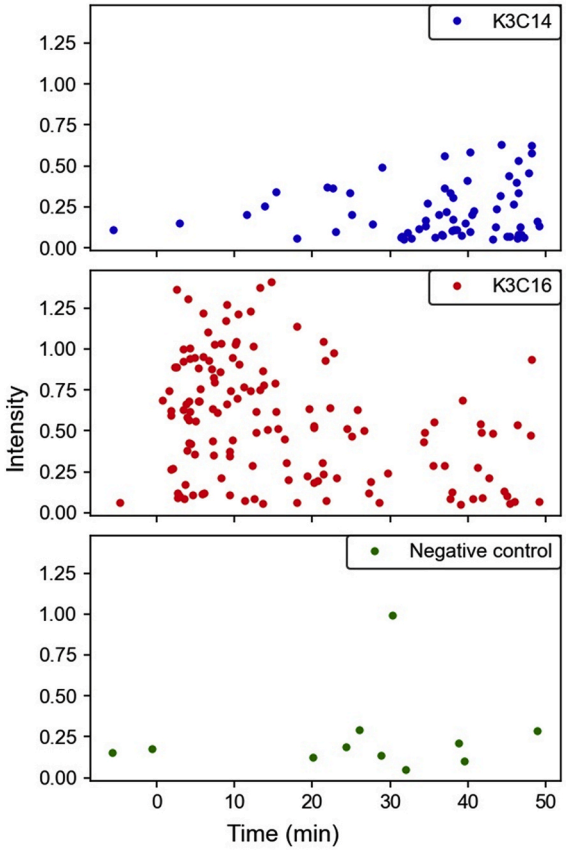

Fig. 4. Peaks of calcium response from all cells of one trial.
Peaks of calcium response were detected in all cells in one field of view (K3C14: 39 cells, K3C16: 47 cells, negative control: 31 cells) and were summarized.

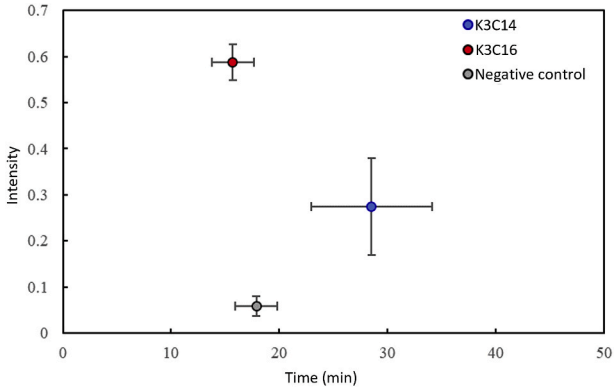

Fig. 5. Averaged peak of calcium response (n = 3, mean ± s.d.).
The time and intensity of the peaks detected in one experiment was averaged for three experiments.

4. Discussion

Membrane-fusogenic liposomes were clarified to interact with the plasma membrane after a few minutes of stimulation [17]. Observation under a confocal microscope revealed images of stained plasma membrane after fluorescent-labeled cationic liposomes were added to the cells. The time course of this membrane fusion process was consistent with that of the calcium response induced by unlabeled K3C16 liposomes, inferring that the phenomenon of membrane fusion was correlated with the calcium response that occurred in the first few minutes. Since there was no use of additional fluorophore-labeling lipids, it could be confirmed that K3C16 liposomes themselves induced membrane fusion. In contrast, the different calcium influx induced by K3C14 liposomes was suggested to correspond to endocytosis. Thus, calcium imaging could be used to evaluate the difference between membrane fusion and endocytosis. Since lipid membranes are not fluorescently labeled, there is no need to consider the effects of amphiphilic

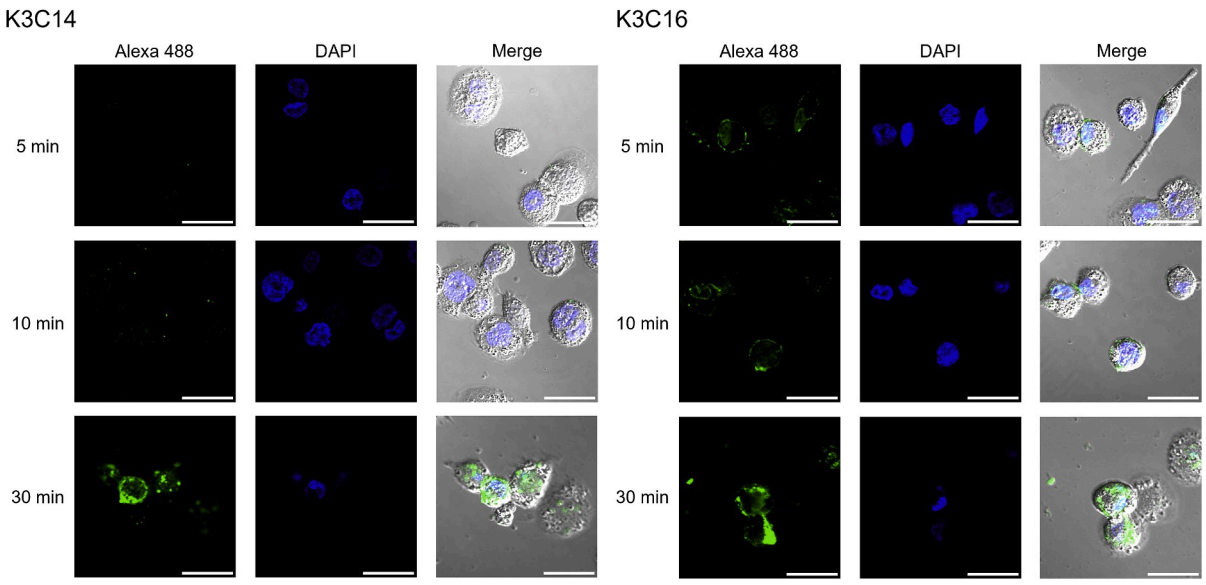

Fig. 6. Fluorescent image of PMA-primed THP-1 cells after stimulated by K3C14 and K3C16 liposomes labeled with Alexa fluor 488™ (scale bar: 30 μm). Fluorescent-labeled liposomes (final concentration 100 μM) were added to PMA-primed (final concentration 100 nM, 18 h) THP-1 cells for 5, 10, and 30 min. After washing, the cells were fixed, stained with DAPI, and observed under a confocal microscope.

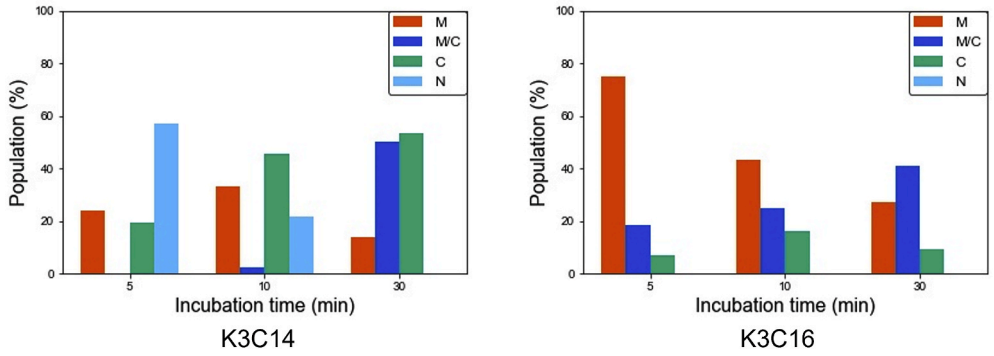

Fig. 7. Intracellular distribution of Alexa fluor 488™ in PMA-primed THP-1 cells.
Cells photographed by confocal microscopy were classified into four categories based on the localization of fluorescent-labeled lipids. (M: cells with the stained plasma membrane, M/C: cells with the stained plasma membrane and cytoplasm, C: cytoplasm stained, N: not stained).

fluorescent substances on promoting membrane fusion. The absence of amphiphilic fluorescent substances makes it possible to evaluate membrane fusion with the original composition of the liposome as it is. Other liposomes that fuse with the plasma membrane in a previous study [3] (DOTAP/DOPE/DiR = 1/1/0.05 (molar ratio)) also caused transient calcium response after the addition of liposomes to the cells, while liposomes introduced into cells by endocytosis (DOTAP/DOPC/DiR = 1/1/0.05 (molar ratio)) caused repeated calcium response (Fig. S4). These data might show that membrane fusion is the trigger of transient calcium response just after the addition of liposomes.

K3C14 liposomes were reported to be taken up by endocytosis and induced lysosome rupture [5]. Also, calcium concentrations in lysosomes are around 500 μM [18]. Therefore, calcium would be released from endosomes or lysosomes into the cytosol by lysosome rupture. The calcium concentration is then thought to decrease as calcium is collected to ER by sarco/endoplasmic reticulum Ca^{2+}-ATPase (SERCA). Since lysosome rupture occurs sporadically, the calcium peaks would be observed randomly. On the other hand, K3C16 liposomes were reported to fuse with the plasma membrane [5,6]. Ion channels on the plasma membrane might open after membrane fusion to allow calcium ions to flow into the cytoplasm from outside the cell. Cytosolic calcium would be pumped into ER by SERCA, resulting in a decrease in cytosolic calcium concentration. Although the mechanism of calcium influx has not been clarified in this study, discovering this mechanism would allow for control of the calcium response that occurs in response to membrane fusion and the subsequent cellular response.

A unique feature of this method is the ability to detect different cell behavior toward liposomes when measuring cellular internalization via endocytosis or membrane fusion. Since individual cells are observed in this method, it is possible to tell differences if the response to liposomes differs from cell to cell; however, a microplate assay would acquire averaged fluorescence intensities of cells, which would not allow analyzing individual cell differences. As such, sporadic calcium response induced by endocytosis could be observed by detecting the responses of individual cells in this study.

The intensity of calcium response from cells was analyzed in previous studies in which charged liposomes were introduced into cells [19]. Manohar et al. stimulated HeLa cells with norepinephrine at different concentrations, and each cell response was classified [20]. In their study, some combinations did not show significant differences between concentrations when the number of peaks and maximum intensity were used as parameters because the time information was lost. We showed that membrane-fusogenic liposomes induced a calcium response immediately after addition by using the time and intensity at which the

peak was detected as parameters. If membrane fusion is a phenomenon triggered by the electrostatic interaction between cationic liposomes and the plasma membrane, then membrane fusion is likely to occur more immediately after the addition of liposomes. The time of the peak of the calcium response could be useful for the detection of membrane fusion. It is expected that the model will be created based on peaks and intensities by machine learning to determine whether the liposomes used in the experiment are introduced into cells via endocytosis or membrane fusion.

In experiments in which liposomal lipids are fluorescent-labeled and their dynamics are observed with confocal microscopy, it is difficult to remove the fluorescence derived from suspended liposomes unless the liposomes are washed. Therefore, it is hard to follow the time course in detail. By using a calcium indicator, it is possible to indirectly follow the membrane fusion process through time-lapse imaging. This makes it possible to observe the cells without determining the stimulation time before observation. Thus the behavior of membrane-fusogenic liposomes can be evaluated with high time resolution without fluorescent labeling. Since membrane fusion is a phenomenon that occurs in a few minutes, it is meaningful to use a calcium indicator with high time resolution to track membrane fusion without fluorescent labeling.

This method is simpler than conventional methods because it does not involve the processes of washing, fixing, or staining cell organelles. Therefore, it is expected to enable the studies of finely tuned liposome concentrations, components of liposomes, and composition ratios on affecting liposome-cell interaction. It is expected to be used as an evaluation system for high-throughput screening. Liposomes can be prepared by microfluidic devices [21]. Therefore, if it becomes possible to prepare liposomes by microfluidic devices, introduce them from devices into cells directly, and determine membrane-fusogenic liposomes from their calcium response, the effort required to find the candidate of membrane-fusogenic liposomes will be substantially reduced compared to conventional methods.

This study takes 60 min to obtain images for one trial. Since the images cannot be obtained simultaneously, it is still time-consuming to test many kinds of liposomes. However, membrane fusion occurs in a few minutes; if a model can be created to determine the time course of membrane fusion based on images taken in a shorter period, the observation time will be further shortened. Within this time frame, this method can be used to rapidly search for membrane-fusogenic liposomes and the effect of lipid composition and size of liposomes on membrane fusion.

5. Conclusion

In this experiment, liposomes taken up via endocytosis and membrane fusion were compared by calcium response. The addition of membrane-fusogenic liposomes produced a strong transient peak immediately. Stimulation with fluorescent-labeled membrane-fusogenic liposomes for the same time as the calcium response appeared confirmed that they interacted with the plasma membrane. These results indicate that membrane fusion and calcium response correspond to each other. This technique is expected to reduce the time and effort required to evaluate membrane fusion and to be used in searching for membrane-fusogenic liposomes.

Funding

This work was partly supported by Top Global University Project by the Ministry of Education, Culture, Sports, Science and Technology (MEXT) of Japan, Grant-in-Aid for Scientific Research (C) (20K12656) by JSPS, Waseda University Grant for Special Research Projects (2018B-214), and Grant-in-Aid for Early-Career Scientists (19K20700) by JSPS.

Declaration of competing interest

The authors declare the following financial interests/personal relationships which may be considered as potential competing interests: S. T. is an inventor of JP 5403324 (Waseda U) for the lysine type lipids.

Acknowledgments

The authors are grateful to Prof. T. Inoue and Dr. C. Adachi from Waseda University for the help and use of their inverted fluorescence microscopy. We acknowledge Prof. T. Oshima, Prof. T. Asahi, and Ms. J. He, also from Waseda University, for their meaningful comments on our research.

Appendix A. Supplementary data

Supplementary data to this article can be found online at https://doi.org/10.1016/j.bbrep.2023.101483.

References

[1] M. Saeed, S. Zalba, A. Seynhaeve, R. Debets, T.L.M. ten Hagen, Liposomes targeted to MHC-restricted antigen improve drug delivery and antimelanoma response, Int. J. Nanomed. 14 (2019) 2069–2089, https://doi.org/10.2147/IJN.S190736.
[2] H. Kong, K. Yi, C. Zheng, Y.-H. Lao, H. Zhou, H.F. Chan, H. Wang, Y. Tao, M. Li, Membrane-fusogenic biomimetic particles: a new bioengineering tool learned from nature, J. Mater. Chem. B (2022), https://doi.org/10.1039/D2TB00632D.
[3] R. Kolašinac, C. Kleusch, T. Braun, R. Merkel, A. Csiszár, Deciphering the functional composition of fusogenic liposomes, Int. J. Mol. Sci. 19 (2) (2018) 346, https://doi.org/10.3390/ijms19020346.
[4] T. Li, J. He, G. Horvath, T. Próchnicki, E. Latz, S. Takeoka, Lysine-containing cationic liposomes activate the NLRP3 inflammasome: effect of a spacer between the head group and the hydrophobic moieties of the lipids, Nanomed. Nanotechnol. Biol. Med. 14 (2) (2018) 279–288, https://doi.org/10.1016/j.nano.2017.10.011.
[5] J. He, T. Li, T. Próchnicki, G. Horvath, E. Latz, S. Takeoka, Membrane fusogenic lysine type lipid assemblies possess enhanced NLRP3 inflammasome activation potency, Biochem. Biophys. Rep. 18 (2019), 100623, https://doi.org/10.1016/j.bbrep.2019.100623.
[6] M. Takikawa, M. Fujisawa, K. Yoshino, S. Takeoka, Intracellular distribution of lipids and encapsulated model drugs from cationic liposomes with different uptake pathways, Int. J. Nanomed. 15 (2020) 8401–8409, https://doi.org/10.2147/IJN.S267638.
[7] B. Dutta, R.K. Arya, R. Goswami, M.O. Alharbi, S. Sharma, S.O. Rahaman, Role of macrophage TRPV4 in inflammation, Lab. Invest. 100 (2) (2020) 178–185, https://doi.org/10.1038/s41374-019-0334-6.
[8] R. Bagur, G. Hajnóczky, Intracellular Ca2+ sensing: role in calcium homeostasis and signaling, Mol. Cell. 66 (6) (2017) 780–788, https://doi.org/10.1016/j.molcel.2017.05.028.
[9] T. Li, F. Tolksdorf, W. Sung, H. Sato, F.J. Eppler, M. Hotta, W. Kolanus, S. Takeoka, Arginine-based cationic liposomes accelerate T cell activation and differentiation in vitro, Int. J. Pharm. 623 (2022), 121917, https://doi.org/10.1016/j.ijpharm.2022.121917.
[10] Y. Obata, S. Saito, N. Takeda, S. Takeoka, Plasmid DNA-encapsulating liposomes: effect of a spacer between the cationic head group and hydrophobic moieties of the lipids on gene expression efficiency, Biochim. Biophys. Acta BBA - Biomembr. 1788 (5) (2009) 1148–1158, https://doi.org/10.1016/j.bbamem.2009.02.014.
[11] C. Adachi, N. Kakinuma, S.H. Jo, T. Ishii, Y. Arai, S. Arai, T. Kitaguchi, S. Takeda, T. Inoue, Sonic hedgehog enhances calcium oscillations in hippocampal astrocytes, J. Biol. Chem. 294 (44) (2019) 16034–16048, https://doi.org/10.1074/jbc.RA119.007883.
[12] C. Adachi, S. Otsuka, T. Inoue, Cholesterol-induced robust Ca oscillation in astrocytes required for survival and lipid droplet formation in high-cholesterol condition, iScience 25 (10) (2022), 105138, https://doi.org/10.1016/j.isci.2022.105138.
[13] T. Inoue, TI Workbench, an integrated software package for electrophysiology and imaging, Microscopy 67 (3) (2018) 129–143, https://doi.org/10.1093/jmicro/dfy015.
[14] Z.-Z. Yang, J.-Q. Li, Z.-Z. Wang, D.-W. Dong, X.-R. Qi, Tumor-targeting dual peptides-modified cationic liposomes for delivery of SiRNA and docetaxel to gliomas, Biomaterials 35 (19) (2014) 5226–5239, https://doi.org/10.1016/j.biomaterials.2014.03.017.
[15] B.R. McNaughton, J.J. Cronican, D.B. Thompson, D.R. Liu, Mammalian cell penetration, SiRNA transfection, and DNA transfection by supercharged proteins, Proc. Natl. Acad. Sci. USA 106 (15) (2009) 6111–6116, https://doi.org/10.1073/pnas.0807883106.
[16] S.R. Sarker, M. Takikawa, S. Takeoka, Vitro delivery of cell impermeable phallotoxin using cationic liposomes composed of lipids bearing lysine headgroup, ACS Appl. Bio Mater. 3 (4) (2020) 2048–2057, https://doi.org/10.1021/acsabm.9b01167.

[17] B. Kim, S. Sun, J.A. Varner, S.B. Howell, E. Ruoslahti, M.J. Sailor, Securing the payload, finding the cell, and avoiding the endosome: peptide-targeted, fusogenic porous silicon nanoparticles for delivery of SiRNA, Adv. Mater. 31 (35) (2019), 1902952, https://doi.org/10.1002/adma.201902952.

[18] W.-A. Wang, L.B. Agellon, M. Michalak, Organellar calcium handling in the cellular reticular network, Cold Spring Harbor Perspect. Biol. 11 (12) (2019), a038265, https://doi.org/10.1101/cshperspect.a038265.

[19] Z. Zhong, Y. Zhai, S. Liang, Y. Mori, R. Han, F.S. Sutterwala, L. Qiao, TRPM2 links oxidative stress to NLRP3 inflammasome activation, Nat. Commun. 4 (1) (2013) 1–11, https://doi.org/10.1038/ncomms2608.

[20] K. Manohar, S. Gare, S. Chel, V. Dhyani, L. Giri, Quantitative confocal microscopy for grouping of dose–response data: deciphering calcium sequestration and subsequent cell death in the presence of excess norepinephrine, SLAS Technol. Transl. Life Sci. Innov. 26 (5) (2021) 454–467, https://doi.org/10.1177/24726303211019394.

[21] I. Eş, L.J. Montebugnoli, M.F.P. Filippi, A.A. Malfatti-Gasperini, A. Radaic, M.B. de Jesus, L.G. de la Torre, High-throughput conventional and stealth cationic liposome synthesis using a chaotic advection-based microfluidic device combined with a centrifugal vacuum concentrator, Chem. Eng. J. 382 (2020), 122821, https://doi.org/10.1016/j.cej.2019.122821.

[22] J.O. Eloy, R. Petrilli, D.L. Chesca, F.P. Saggioro, R.J. Lee, J.M. Marchetti, Anti-HER2 immunoliposomes for co-delivery of paclitaxel and rapamycin for breast cancer therapy, Eur. J. Pharm. Biopharm. 115 (2017) 159–167. https://doi.org/10.1016/j.ejpb.2017.02.020.

[23] S.K. Golombek, J.-N. May, B. Theek, L. Appold, N. Drude, F. Kiessling, T. Lammers, Tumor targeting via EPR: strategies to enhance patient responses, Adv. Drug Deliv. Rev. 130 (2018) 17–38. https://doi.org/10.1016/j.addr.2018.07.007.